

MA Jing, WU Chengke, CHEN Dong, ZHOU Youxi

Embedded coding of medical images with regions of interest based on 3-D zerotree

© Higher Education Press and Springer-Verlag 2007

Abstract In order to satisfy the need of diagnoses, based on the characteristic of medical images that a sequence of frames are formed in one body inspection, a new strategy for medical images compression is proposed. The 3-D wavelet is adopted and the planar zerotree is extended to the 3-D zerotree. By making use of the 3-D zerotree structure, a simple method for region of interest (ROI) mask generation is put forward. Medical images are compressed by three-dimensional embedded coding with the compression of regions of interest. Simulation results have shown that it can efficiently improve the compression ratio without affecting the diagnoses.

Keywords 3-D wavelet transform (3DWT), ROI, 3-D zerotree, ROI, embedded zerotree wavelet (EZW), medical image compression

1 Introduction

Redundancy of information is one of the characteristics of the medical images. Medical images are usually created by many medical apparatus, such as computerized tomography (CT), magnetic resonance imaging (MR), positron emission tomography (PET). A sequence of frames is formed in one body inspection, which leads to a special correlation between frames. Unlike the correlation of the frames in video, this correlation is in the dimension of space. Obviously, it is difficult to remove such a special correlation for the usual medical image compression technologies such as joint photographic experts group (JPEG), JPEG2000, set partitioning in hierarchical trees (SPIHT) and other video compression methods. To have the medical images from CT and MRI better compressed, a novel strategy is proposed in this paper. An efficient embedded coding based on 3-D zerotree is designed as well as an easily realized template design method of ROI.

Translated from *Journal of Xidian University*, 2006, 33(2): 182–185
 [译自: 西安电子科技大学学报]

MA Jing (✉), WU Chengke, CHEN Dong, ZHOU Youxi
 State Key Laboratory of Integrated Service Networks, Xidian University, Xi'an 710071, China
 E-mail: jingma@mail.xidian.edu.cn

2 3-D wavelet transform

In 1989, the wavelet was first introduced into the signal processing by Mallat [1]. Information in the images is decomposed into different frequency channels by the wavelet. According to the correlation in space dimension between frames from those images sequence created by CT and MRI, 3-D wavelet [2] is used in our algorithm. The procedure of the 3-D wavelet in medical images is as follows.

A 2-D wavelet is first applied in every frame. And then a third wavelet is used in Z axis (the dimension between frames) for those coefficients previously obtained in each frame. It can be realized like the following.

For an arbitrary 3-D signal $f(x, y, z) \in V_{J_1}^3$, assume the sequence $\{c_{J, m_1, m_2, m_3}, m_1, m_2, m_3 \in Z\} \in I^3$. Let $L = (L_{m,k})$, $H = (H_{m,k})$, where $L_{m,k} = l_{k-2m}$, $H_{m,k} = h_{k-2m}$. L_x, L_y, L_z indicate the effects of L on the signal in x, y, z axis. And H_x, H_y, H_z indicate the effects of H on the signal in x, y, z axis. Then we will get

$$\begin{aligned} f(x, y, z) &= \sum C_{J_{j+1}} \Phi^3(x, y, z) + \sum_{j=J_1+1}^{J_2} \sum_{n=1}^7 D_j^n f(x, y, z) \\ &= A_{J_2} f(x, y, z) + \sum_{j=J_1+1}^{J_2} \sum_{n=1}^7 D_j^n f(x, y, z) \end{aligned} \quad (1)$$

$$\text{and } \begin{cases} C_{j+1} = L_x L_y L_z C_j \\ D_{j+1}^n = Q^n C_j, \quad j = J_1, J_1 + 1, \dots, J_2 \end{cases} \quad (2)$$

where $\Phi^3(x, y, z) = \varphi(x)\varphi(y)\varphi(z)$ is a function that can be decomposed in three dimension, and Q^n is a combination L_x, L_y, L_z, H_x, H_y .

It is shown that A_{J_2}, D_j^n can separately indicate the weight of low frequency and high frequency, which is similar to those in the 2-D Mallet decomposition.

Equations (1) and (2) is the algorithm of the decomposition in 3-D wavelet. And then the composition method can be gotten (* indicates conjugate)

$$C_j = L_x^* L_y^* L_z^* C_{j+1} + \sum_{n=1}^7 Q^{n*} C_{j+1}, \quad j = J_2 - 1, J_2 - 2, \dots, J_1 \quad (3)$$

3 3-D embedded zerotree wavelet based on ROI

The embedded zerotree wavelet proposed by Shapiro [3,4] is based on the strong correlation between the coefficients in each layer after wavelet. If a coefficient in low frequency is less than a certain threshold, its corresponding coefficients in high frequency are quite likely less than this threshold. This special data structure is named “zerotree.” The embedded zerotree wavelet from Shapiro is suitable for the 2-D signal. In this paper, the embedded zerotree wavelet is extended to 3-D based on the 3-D wavelet to satisfy the processing of 3-D signals in medical images.

3.1 3-D zerotree prediction

A tree structure is formed by arranging the coefficients from low frequency to high frequency after 3-D wavelet of a sequence of medical images [5]. The root is the crunode with the lowest frequency. Its 7 children locate in each corresponding sub-lowest frequency position. All the other subbands except the subbands with the highest frequency have 8 children. It is shown in Fig. 1, which is a tree with the depth of 4.

And then a data structure of 3-D zerotree can be defined: each wavelet coefficient x corresponds to a threshold T . If $|x| < T$, then x is considered to be unimportant. If a coefficient is considered to be unimportant according to a given threshold T in a large scale, then all the coefficients in the same space in a smaller scale are also considered to be unimportant.

These unimportant coefficients form a zerotree. The position information to describe the important coefficients ($|x| \geq T$) is largely reduced by these zerotrees.

The mathematical description of the 3-D zerotree can be expressed as

$$\text{Tree}(x, y, m, s) = \left\{ \begin{array}{l} \{(x, y, z, m, s)\} \cup \text{Tree}(2x, 2y, 2z, m-1, s) \\ \cup \text{Tree}(2x+1, 2y, 2z, m-1, s) \\ \cup \text{Tree}(2x, 2y+1, 2z, m-1, s) \\ \cup \text{Tree}(2x, 2y, 2z+1, m-1, s) \\ \cup \text{Tree}(2x+1, 2y+1, 2z, m-1, s) \\ \cup \text{Tree}(2x+1, 2y, 2z+1, m-1, s) \\ \cup \text{Tree}(2x, 2y+1, 2z+1, m-1, s) \\ \cup \text{Tree}(2x+1, 2y+1, 2z+1, m-1, s), \\ \quad m \neq 1 \text{ and } s \neq \text{LLL} \\ \{(x, y, z, m, \text{LLL})\} \cup \text{Tree}(x, y, z, m, \text{HLL}) \\ \cup \text{Tree}(x, y, z, m, \text{LHL}) \\ \cup \text{Tree}(x, y, z, m, \text{HHL}) \\ \cup \text{Tree}(x, y, z, m, \text{LHH}) \\ \cup \text{Tree}(x, y, z, m, \text{HHH}), \quad m = M \text{ and } s = \text{LLL} \\ \{(x, y, z, m, s)\}, \quad m = 1 \end{array} \right. \quad (4)$$

where x, y, z indicates the 3-D position of the coefficients in the sub-image. m indicates the layer of the sub-image (1, 2, ..., M). s indicates the direction of the sub-image (LLL, LLH, LHL, LHH, HLL, HLH, HHL, HHH).

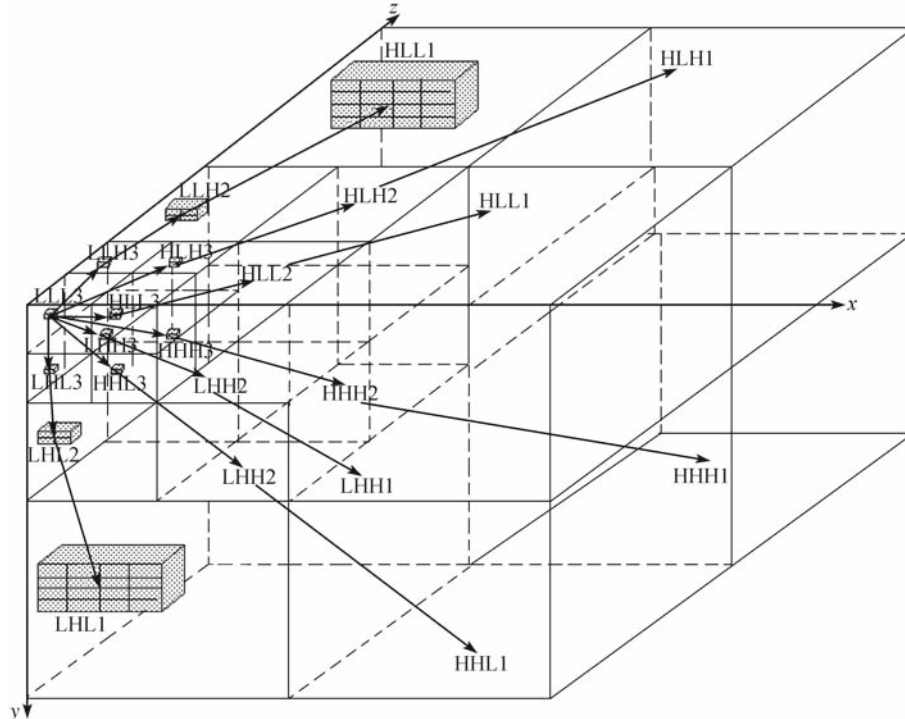


Fig. 1 Structure of the 3-D zerotree

as $\{(x_1^b, y_1^b, z_1^b), (x_2^b, y_2^b, z_2^b)\}$, shown in Fig. 2(b). Then we will get

$$\begin{cases} x_1^b = \left\lfloor \frac{x_1}{2} \right\rfloor, & y_1^b = \left\lfloor \frac{y_1}{2} \right\rfloor, & z_1^b = \left\lfloor \frac{z_1}{2} \right\rfloor \\ x_2^b = \left\lfloor \frac{x_2}{2} \right\rfloor, & y_2^b = \left\lfloor \frac{y_2}{2} \right\rfloor, & z_2^b = \left\lfloor \frac{z_2}{2} \right\rfloor \end{cases} \quad (5)$$

where b is the type of the subband. If several wavelets are applied, $\{(x_1^{\text{LL}_1}, y_1^{\text{LL}_1}, z_1^{\text{LL}_1}), (x_2^{\text{LL}_1}, y_2^{\text{LL}_1}, z_2^{\text{LL}_1})\}$ can be obtained. According to Eq. (5) the ROI of the other subbands $\{\text{LLL}_2, \text{HLL}_2, \text{LHL}_2, \text{LLH}_2, \text{HHL}_2, \text{HLH}_2, \text{LHH}_2, \text{HHH}_2\}$ can be calculated.

3.3 The sequence of the 3-D zerotree coding in significance map

The significance map contains three elements, significant pixels, zero outlier and zerotree root. To improve the embedded coding, the symbols of significant pixels and the significance map are coded together. Because the coding of 3-D zerotree is similar to the 2-D zerotree, only the scan sequence of the coding is pointed out here, shown in Fig. 3. The parent band should be scanned before its subbands, and the next subband can be scanned only after the end of the scan of the current subband.

4 Simulation results

A set of CT images of lung cancer is used in our simulation. The parameter of these images is $512 \times 512 \times 24 \times 23$ (length is 512, width is 512, each pixel is expressed in 24 b. The number of the images is 23). The ROI is a cubic of $65 \times 65 \times 23$, with the end points of the body diagonal $\{(95, 225, 0), (160, 290, 23)\}$. The results are compared with the ROI + 2-D EZW method described in Ref. [4]. The bit-plane scaling is used in the ROI processing.

The power signal-to-noise ratio (PSNR) of the representational frames is shown in Tables 1 and 2. The compression ratio is 8, 16, 32 and 64, and the bit-plane scaling parameter is 4.

Table 1 PSNR of method in Ref. [4]

Frame	Ratio = 8		Ratio = 16		Ratio = 32		Ratio = 64	
	ROI	BG	ROI	BG	ROI	BG	ROI	BG
1st	53.60	49.12	50.93	47.33	45.18	41.56	40.91	37.65
11th	53.46	48.66	49.36	45.51	43.83	39.42	38.74	34.46
21st	53.16	48.29	49.63	45.56	44.26	39.89	39.55	34.75

Table 2 PSNR of our method

Frame	Ratio = 8		Ratio = 16		Ratio = 32		Ratio = 64	
	ROI	BG	ROI	BG	ROI	BG	ROI	BG
1st	55.12	50.46	52.45	48.03	46.78	42.66	42.23	38.55
11th	55.01	49.76	50.46	46.11	45.13	40.22	39.94	35.20
21st	54.76	49.39	50.89	46.65	45.96	40.03	40.86	36.08

Figures 4 and 5 show the results of the 11th frame after the 8-times compression.

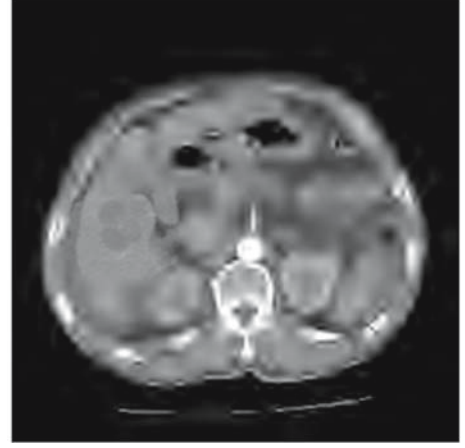


Fig. 4 Result of method in Ref. [7]

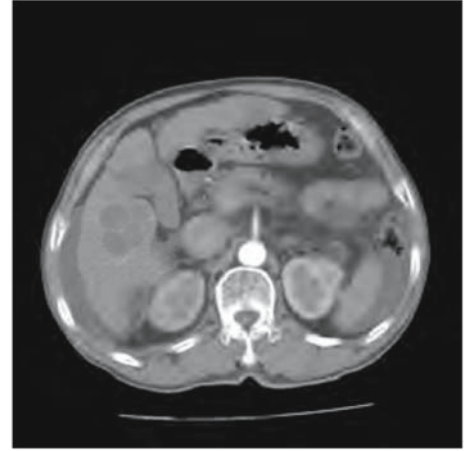


Fig. 5 Result of our method

Figures 6 and 7 are a performance comparison of the 11th frame after a 64 times compression.

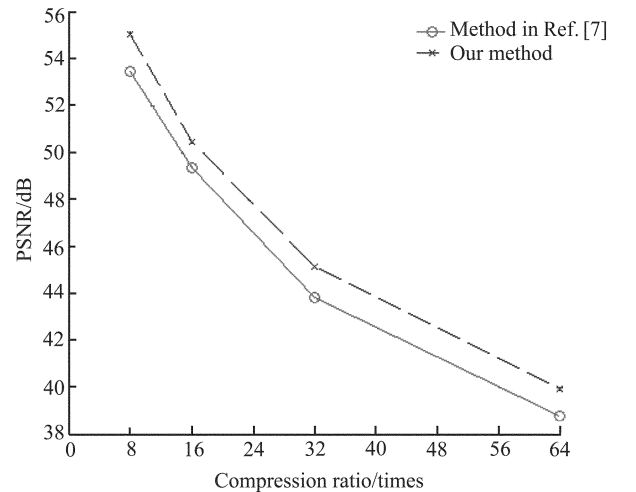


Fig. 6 PSNR comparison between our method and method in Ref. [7]

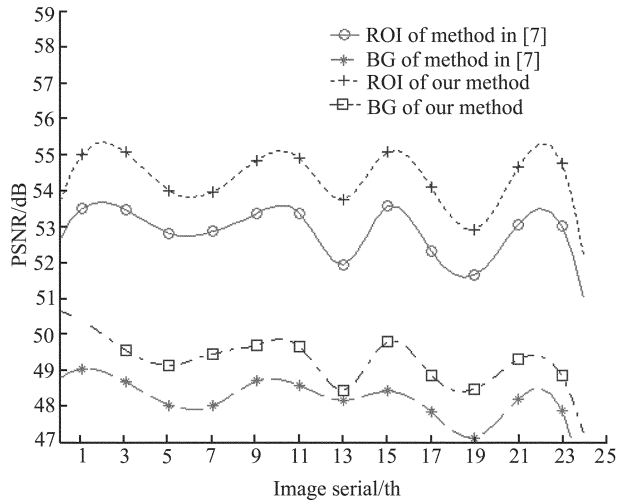


Fig. 7 PSNR comparison of ROI and BG between our method and method in Ref. [7] with ratio 8

With the coding of ROI, our method can achieve 1–2 dB improvement in PSNR compared with the method in Ref. [7], and the improvement in background is about 1 dB.

5 Conclusions

In this paper, the 3-D wavelet is introduced in the compression of medical images according to the characteristic of medical images. The 2-D embedded zerotree wavelet is

extended to 3-D. Based on the ROI coding, a new medical images compression strategy, which is 3-D wavelet + ROI coding + 3-D embedded zerotree wavelet, is proposed. Simulation results have shown that the PSNR achievement can be 1–2 dB.

Acknowledgements This work was supported by the National Natural Science Foundation of China (Grant No. 60272050).

References

1. Mallat S A. Theory for multiresolution signal decomposition: The wavelet representation. *IEEE Trans. on Pattern Anay, Mach I Intel*, 1989, 11 (7): 674–693
2. Zhang Wenzhong, Shen Lansun.. Image coding using a new 3-D wavelet transform scheme. *Acta Electronica Sinica*, 1997, 25 (10): 32–36 (in Chinese)
3. Shapiro J M. Smart compression using the embedded zerotree wavelet (EZW) algorithm. In: *Proceedings of the 27th Asilomar Conference on Signals, Systems & Computers*. Pacific Grove: IEEE, 1993, 486–490
4. Shapiro J M. Embedded image coding using zerotrees of wavelet coefficients. *IEEE Trans on Signal Processing*, 1993, 41 (12): 3445–3462
5. Li Hui. Medical image compression based on three dimensional wavelet transformation in PACS. *Journal of Image and Graphics*, 2000, 5(2): 114–118 (in Chinese)
6. Agraflois D. Three-dimensional coding of volumetric medical images using of interest, *Visual Information Engineering*. IEE, Stevenage: Michael Faraday House, 2003, 194–197
7. Chen Jun, Wu Chengke, Li Yunsong. Embedded coding of images with regions of interest based on zerotree. *Journal of Xidian University*, 2002, 29 (3): 343–346 (in Chinese)